Archives of Biochemistry and Biophysics 486 (2009) 88–93

Contents lists available at ScienceDirect

Archives of Biochemistry and Biophysics

journal homepage: www.elsevier.com/locate/yabbi

Inhibition of uncoupling protein 2 by genipin reduces insulin-stimulated glucose uptake in 3T3-L1 adipocytes

Hui Zhou, Jing Zhao, Xujia Zhang *

National Laboratory of Biomacromolecules, Institute of Biophysics, Chinese Academy of Sciences, 15 Datun Road, Chaoyang District, Beijing 100101, China

ARTICLE INFO

Article history:
Received 30 December 2008
and in revised form 26 February 2009
Available online 9 March 2009

Keywords:
3T3-L1
Glucose uptake
Insulin resistance
Reactive oxygen species
Uncoupling protein

ABSTRACT

Uncoupling protein 2 (UCP2) was reported to be involved in insulin–glucose homeostasis, based on well established event that inhibition of UCP2 stimulates insulin secretion in pancreatic β-cells. However, the role of UCP2 on insulin-stimulated glucose uptake in adipose tissue, which is an indispensable process in insulin–glucose homeostasis, remains unknown. In this study, UCP2 was inhibited by genipin in 3T3-L1 adipocytes, which increased mitochondrial membrane potential, intracellular ATP level and production of reactive oxygen species (ROS). Importantly, insulin-stimulated glucose uptake in 3T3-L1 adipocytes was largely impaired in the presence of genipin, and recovered by CCCP, a mitochondrial uncoupler. Furthermore, genipin leaded to suppression of insulin signal transduction through hyperactivation of c-Jun N-terminal kinase (JNK) and subsequent serine phosphorylation of insulin receptor substrate-1 (IRS-1). These results suggest that mitochondrial uncoupling in adipocytes positively regulates insulin-stimulated glucose uptake in adipocytes, and UCP2 may play an important role in insulin resistance.

© 2009 Elsevier Inc. All rights reserved.

Plasma glucose is tightly controlled by insulin–glucose homeostasis. Elevated plasma glucose induces insulin secretion from pancreatic β-cells, which can stimulate glucose uptake into skeletal muscle and adipose tissue, and decrease glucose production in liver [1]. Reduced ability of insulin to regulate glucose homeostasis in these tissues (skeletal muscle, adipose tissue and liver) causes insulin resistance, which is believed to be an early feature of type 2 diabetes [2,3]. However, the mechanism responsible for insulin resistance is largely unknown.

Uncoupling proteins (UCPs)[1] belong to a large family of mitochondrial anion carrier proteins. Three homologs, UCP1, UCP2 and UCP3 have been identified in various tissues [4]. It has been well documented that UCPs function to mediate proton leak across the mitochondrial inner membrane so that the inner membrane potential generated from respiration chain is dissipated rather than producing ATP [4–8].

UCP2 is widely expressed, mainly in pancreas, immune system, white adipose tissue, and the brain [9]. Unlike UCP1, which is restricted to expression in brown adipose tissue and plays an important role in thermogenesis [10,11], the physiological roles of UCP2 is still unclear. Overexpression of UCP2 shows protection potential from oxidative damage by modulating mitochondrial reactive oxygen species (ROS) production [12,13]. Recently, UCPs were also reported to be involved in the control of insulin–glucose homeostasis [14–21]. In the regulation of insulin–glucose homeostasis, UCP2 was identified as a negative regulator of insulin release from studies in pancreatic β-cells from UCP2-null mice [14,20,21]. However, whether UCP2 regulates insulin-stimulated glucose uptake into white adipose tissue has not been studied.

Genipin was discovered to be an effective inhibitor of UCP2, and used successfully for the functional studies of UCP2 in pancreatic β-cells [21] and neurons [19]. In this study, by inhibiting UCP2 with genipin, the effect of UCP2 on insulin-stimulated glucose uptake in 3T3-L1 adipocytes was investigated. Our results show that inhibiting UCP2 decreases insulin-stimulated glucose uptake in 3T3-L1 adipocytes. Moreover, inhibiting UCP2 induces increases in mitochondrial potential and ATP production, and enhances the production of ROS, which may be associated with insulin resistance in adipocytes.

Materials and methods

Materials

Genipin was purchased from WaKo Pure Chemical Industries. Antiserum to phospho-Ser473 of Protein kinase B (PKB/Akt) obtained from Signalway Antibody Co., Ltd. (SAB). Other antiserum and antibodies were purchased from Cell Signaling. 2-deoxy-D-[1,2-^{3}H] glucose ([^{3}H]-2-DG) was purchased from PerkinElmer.

* Corresponding author. Fax: +86 10 6487 2026.
E-mail address: xjzhang@sun5.ibp.ac.cn (X. Zhang).

[1] *Abbreviations used:* UCPs, uncoupling proteins; ROS, reactive oxygen species; PKB, protein kinase B; DMEM, Dulbecco's modified Eagle's medium; NCS, newborn calf serum; FBS, fetal bovine serum; PBS, phosphate buffered saline; ECL, enhanced chemiluminescence; CCCP, carbonyl cyanide 3-chlorophenylhydrazone; IRS-1, insulin receptor substrate-1.

0003-9861/$ - see front matter © 2009 Elsevier Inc. All rights reserved.
doi:10.1016/j.abb.2009.02.017

Dulbecco's modified Eagle's medium (DMEM), newborn calf serum (NCS), fetal bovine serum (FBS) and other cell culture products were from Gibco-BRL. Plasmid pcDNA3.1 and lipofectamine 2000 were obtained from invitrogen. Other chemicals were from Sigma.

Cell culture and transfection

HEK293 cells were cultured in high-glucose DMEM supplemented with 10% (v/v) fetal bovine serum. UCP2 cDNA was subcloned into the EcoRI/XhoI digested vector pcDNA3 to construct vector pcDNA-UCP2. Vectors (pcDNA-empty and pcDNA-UCP2) were transfected into HEK293 by lipofectamine 2000 to build empty cells and UCP2-transfected cells, respectively.

3T3-L1 fibroblasts obtained from Dr. Tao Xu (Beijing, China) were grown and differentiated into 3T3-L1 adipocytes as described [22]. Briefly, 3T3-L1 cells were cultured in high-glucose DMEM supplemented with 10% (v/v) newborn calf serum at 37 °C and 5% CO2. One day after confluence, cells were switched into differentiation medium containing 10% (v/v) fetal bovine serum, 1 μM bovine insulin, 0.5 mM 3-isobutyl-1-methylxanthine, and 0.25 μM dexamethasone. Two days later, the medium was changed to 10% (v/v) fetal bovine serum and 1 μM bovine insulin for another 2 days. Cells were then maintained in DMEM with 10% (v/v) fetal bovine serum. For experiments, cells were used on 9–10 days post-differentiation, at which time more than 90% of the cells exhibited the fatty phenotype as judged by phase-contrast microscopy.

Measurement of glucose transport activity

3T3-L1 adipocytes were starved in serum-free DMEM containing 5 mM glucose for 2 h, then cells were washed and placed in KRBH buffer (25 mM Hepes, 120 mM NaCl, 4.6 mM KCl, 1.9 mM CaCl2, 1 mM MgSO4, 1.2 mM KH2PO4, pH 7.4). After pre-incubated with genipin of various concentrations for 20 min, cells were incubated with or without 100 nM insulin for 20 min at 37 °C. Next, 2-DG (0.1 mM, 0.5 μCi) was added and incubation continued for 5 min at 37 °C, and cells were washed in ice-cold KRBH buffer and lysed in 10% (w/v) Triton X-100. Aliquots were measured for radioactivity by liquid scintillation and luminescence counter (PerkinElmer), and protein content was measured by the BCA method.

Determination of mitochondrial membrane potential

The mitochondrial membrane potential was determined by JC-1 probe as described previously [23]. Cells were digested into sterile centrifuge tubes by trypsin–EDTA solution (Sigma), then washed twice with PBS and resuspended cells in 0.5 ml KRBH buffer containing 1% (w/v) BSA. After pre-incubated with or without genipin for 20 min, cells were incubated with 2 μM JC-1 at 37 °C for 20 min. Then cells were washed twice and resuspended with PBS. Cell fluorescence was measured immediately by fluorescence spectrophotometer (F4500, Hitachi). Mitochondrial membrane potential was determined by ratio of red fluorescence (excitation 550 nm, emission 600 nm) to green fluorescence (excitation 485 nm, emission 535 nm).

Determination of ATP production

3T3-L1 adipocytes were pre-incubated for 30 min in KRBH buffer containing 5 mM glucose and then treated with or without genipin for 1 h. At the end of this incubation, cells were disrupted with lysis buffer on ice. Extracts were centrifuged at 13,000*g* for 15 min at 4 °C and supernatants were collected. ATP was measured using a luciferin-luciferase bioluminescent assay (Sigma). Light emission was recorded for 30 s by photon counting luminometer. Relative ATP level was normalized by protein concentration determined by the BCA method.

Determination of ROS production

Mitochondrial ROS generation was assessed by using dihydrorhodamine 123 (DHR123), which was mitochondrial target probe [24]. Cells were pre-incubation in KRBH buffer containing 5 mM glucose for 20 min, and then treated with or without genipin for 20 min. Then cells were loaded with 5 μM DHR123 for 30 min. After washed with PBS, cells were scraped and disrupted on ice. Fluorescence (excitation 500 nm, emission 535 nm) was then measured immediately. In addition, intracellular ROS was determined by 10 μM DCFH-DA (excitation 495 nm, emission 525 nm) [25] as described above. Protein content was measured by the BCA method. The intensity of fluorescence was expressed as arbitrary units per mg protein.

Western blotting

3T3-L1 adipocytes were pre-incubated with serum-free DMEM containing 5 mM glucose for 2 h, and then cells were washed and placed in KRBH buffer. After treatment, cells were rinsed briefly with ice-cold phosphate buffered saline (PBS), then disrupted in ice-cold lysis buffer at 4 °C. Supernatants were collected following centrifuging at 13,000*g* for 15 min at 4 °C. Proteins concentration was determined by the BCA method. Equivalent amounts of proteins were loaded and separated by SDS–PAGE, and transferred to PVDF membranes (Millipore). After incubation with antibodies, proteins were detected with enhanced chemiluminescence (ECL) system.

Statistical analysis

Experimental data were presented as means ± standard deviation (SD). The data are from three independent experiments with three replicates per experiment. Statistical analysis was made using the Student's t-test. $P < 0.05$ was considered to be significant for a difference.

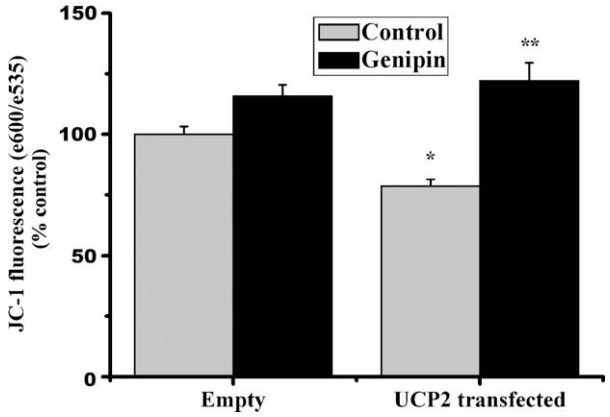

Fig. 1. Genipin increases mitochondrial membrane potential in a UCP2-dependent manner in HEK293. Empty vector transfected (empty) and UCP2-transfected HEK293 cells were harvested and resuspended in KRBH buffer containing 1% BSA. After incubation with genipin (50 μM) at 37 °C for 20 min, cells were loaded with probe JC-1 (2 μM) at 37 °C for 20 min. Data are expressed as 600/535 nm fluorescence ratio and shown as percentage over control of empty cells ± SD of three independent experiments with three replicates per experiment. $^{*}P < 0.05$, significant to control of empty cells. $^{**}P < 0.01$, significant to control of UCP2-transfected cells.

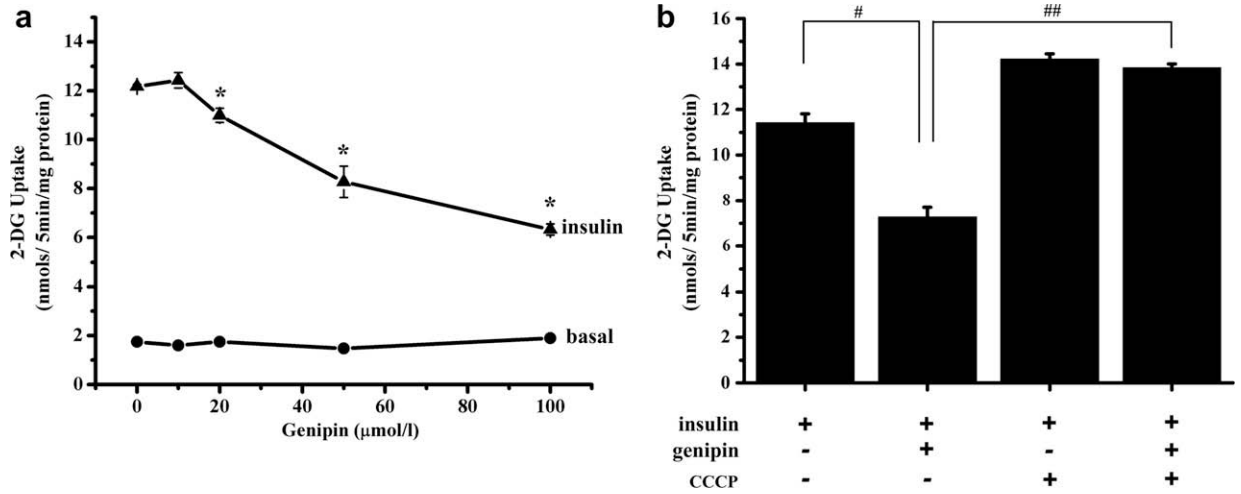

Fig. 2. Insulin-stimulated glucose uptake in 3T3-L1 adipocytes was impaired by genipin and the effect of genipin was blocked by CCCP added simultaneously. (a) Effect of genipin on glucose uptake of 3T3-L1 adipocytes. 2-DG uptake was measured for 5 min under basal (●) or acute insulin stimulation (20 min at 37 °C) with 100 nM insulin (▲) after incubation for 20 min in the presence of genipin at various concentrations. 2-DG uptake was expressed as uptake amount per mg protein in 5 min. (b) As above, insulin-stimulated 2-DG uptake in adipocytes was impaired after cells were pretreated with 50 μM genipin. CCCP could block the reduction of uptake induced by genipin when cells were pretreated with genipin and additional 50 nM CCCP, although CCCP leaded to mildly increase of 2-DG uptake. 2-DG uptake was expressed as uptake amount per mg protein in 5 min. Data are the means ± SD of three independent experiments with three replicates per experiment. $^{*}P < 0.01$, significant to the control (untreated), $^{\#}P < 0.01$, $^{\#\#}P < 0.01$.

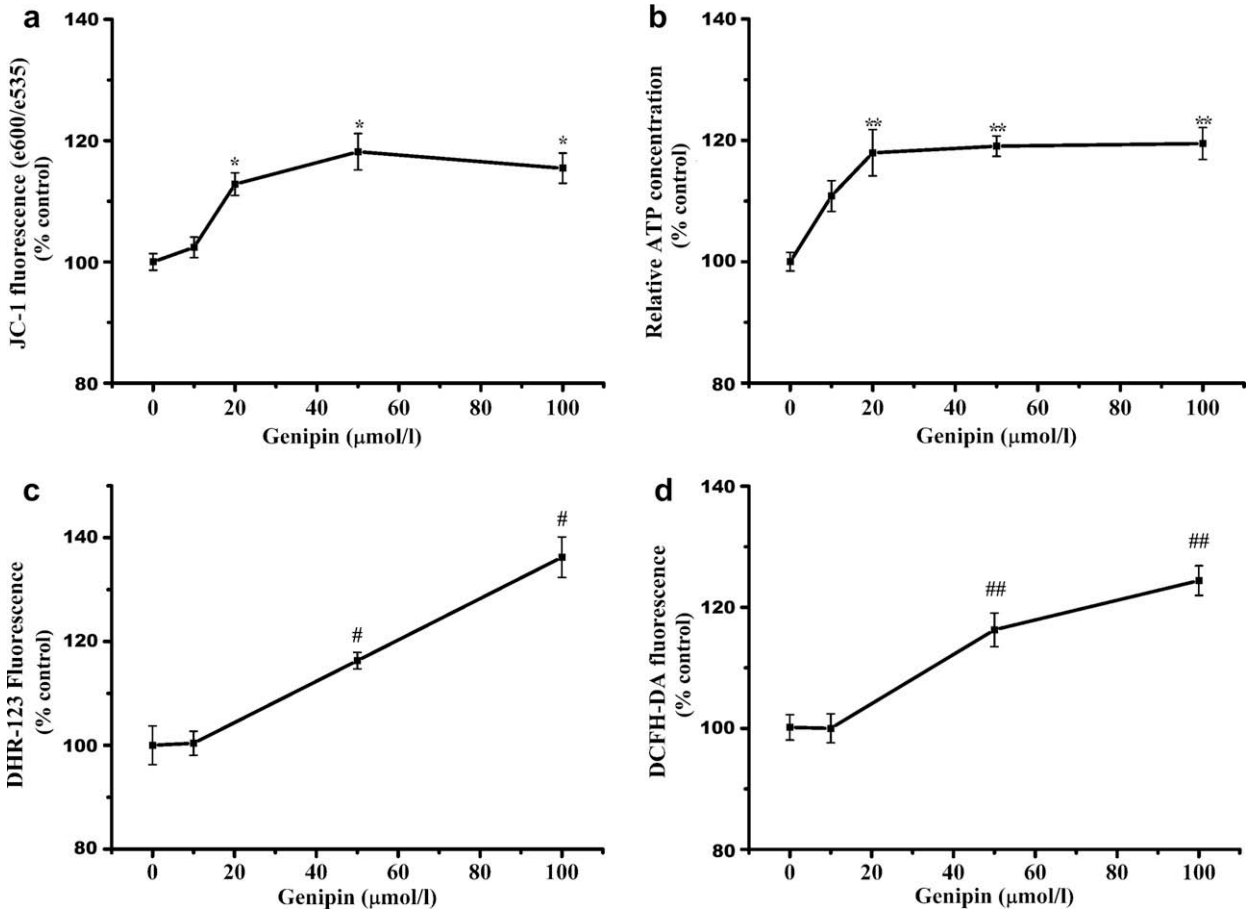

Fig. 3. Effect of genipin on mitochondrial functions in 3T3-L1 adipocytes. (a) Genipin increases mitochondrial membrane potential in adipocytes. Mitochondrial membrane potential of 3T3-L1 adipocytes was measured by JC-1 after incubation at 37 °C for 20 min in the presence of genipin at various concentrations, data were expressed as 600/535 nm fluorescence ratio. (b) Genipin increases intracellular ATP level in adipocytes. Intracellular ATP level was determined by luciferin-luciferase bioluminescent assay after incubation for 1 h in the presence of genipin at various concentrations. (c) Genipin increases mitochondrial and intracellular ROS. Mitochondrial ROS level of 3T3-L1 adipocytes was determined by loading with DHR123 after incubation for 20 min in the presence of genipin at various concentrations. In addition, genipin increases intracellular ROS level (d), determined by loading with DCFH-DA. Data are shown as percentage of control ± SD of three independent experiments with three replicates per experiment. $^{*}P < 0.01$, $^{**}P < 0.01$, $^{\#}P < 0.05$, $^{\#\#}P < 0.05$, significant to control, respectively.

Results

Genipin increases mitochondrial membrane potential by inhibiting activity of UCP2

Genipin, which is a cell permeable molecule, was shown to inhibit UCP2-mediated proton leak by directly interacting with UCP2, and regulate mitochondrial functions from pancreatic β-cells [21]. Our study further demonstrates that genipin was able to inhibit superoxide-activated mitochondrial proton leak and increased mitochondrial membrane potential in a UCP2-dependent manner in kidney (data not shown). In this study, we examined the effect of genipin on mitochondrial membrane potential in UCP2-transfected HEK293 cells. UCP2-transfected cells significantly increased JC-1 fluorescence after treatment with genipin (Fig. 1), compared to non-transfected cells expressing less UCP2. Moreover, UCP2-transfected cells had significant low mitochondrial membrane potential than empty cells (Fig. 1), due to proton leak activity of UCP2. Thus, genipin increased mitochondrial membrane potential in a UCP2-dependent manner, which is consistent with the reports that genipin is an inhibitor of UCP2 [19,21].

Inhibition of UCP2 reduces glucose uptake in 3T3-L1 adipocytes

To test if UCP2 in adipocytes was associated with glucose uptake, insulin-stimulated glucose uptake was measured in 3T3-L1 adipocytes. UCP2 activity was inhibited by genipin, which had been demonstrated by Zhang et al. [21] and our above experi-

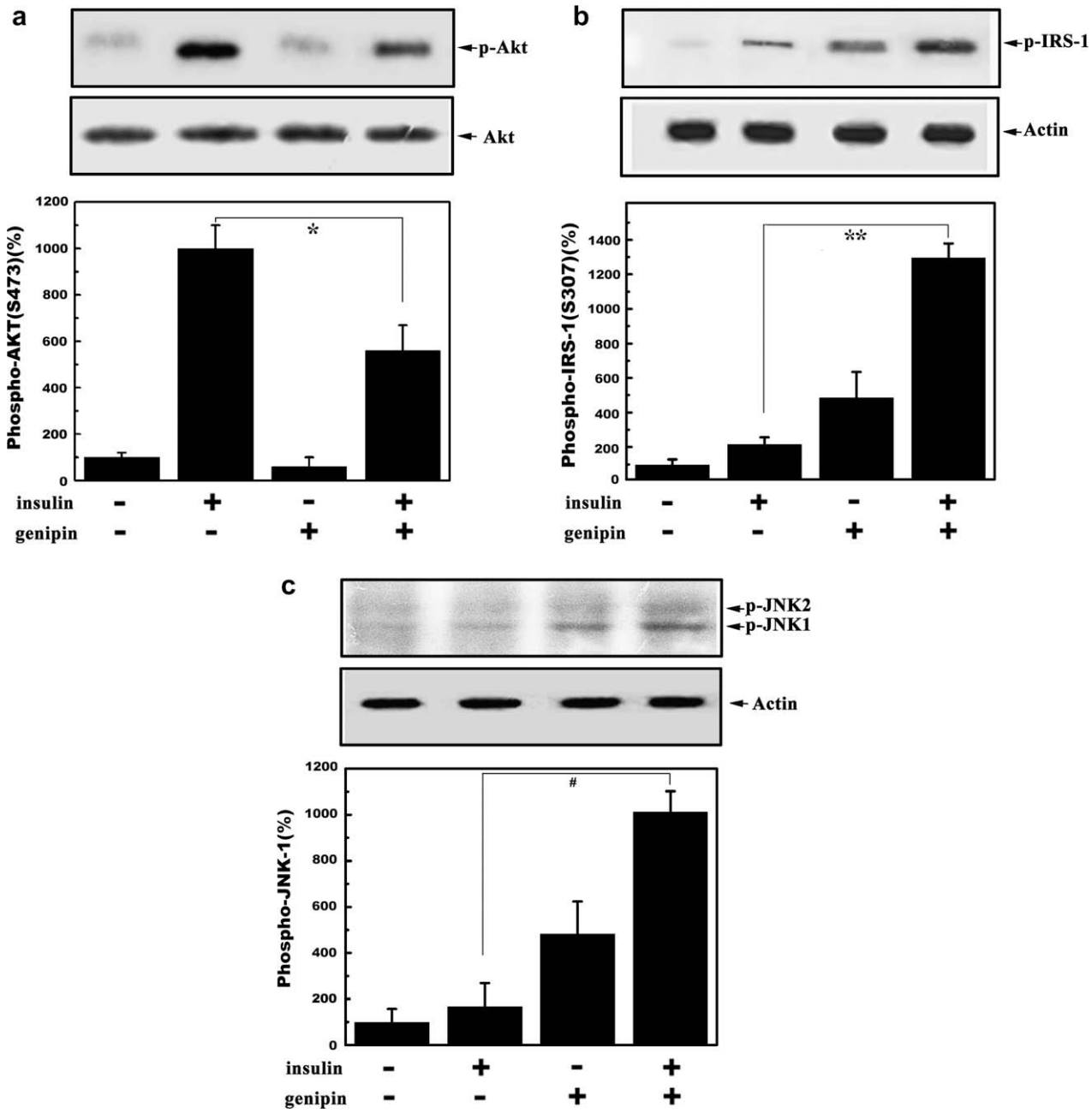

Fig. 4. Effect of genipin on intracellular signaling. Serum- and glucose-starved 3T3-L1 adipocytes were pretreated with 50 μM genipin for 1 h and then stimulated with 100 nM insulin as indicated. Cell lysates were prepared and analyzed by SDS–PAGE and immunoblotting. In the presence of genipin, insulin-induced Akt phosphorylation was suppressed (a), Ser307 phosphorylation of IRS-1 was increased (b), and phosphorylation of JNK1/2 was also increased (c). Data are shown as percentage of control ± SD and are representatives of three independent experiments. $^{*}P < 0.01$, $^{**}P < 0.01$, $^{\#}P < 0.01$.

ments. The result shows that insulin-stimulated glucose uptake was inhibited by as much as 50% in the presence of 100 μM genipin (Fig. 2a). This suggests that the inhibition of mitochondrial proton leak via UCP2 induced insulin resistance in adipocytes. If so, the recovery of mitochondrial proton leak could restore the insulin-stimulated glucose uptake. Therefore, insulin-stimulated glucose uptake was measured in the presence of 50 nM CCCP (carbonyl cyanide 3-chlorophenylhydrazone, a chemical uncoupler that stimulates proton leak). As expected, CCCP protected against the genipin-induced inhibition of insulin-stimulated glucose uptake (Fig. 2b). Our results demonstrated that the inhibition of UCP2 induced insulin resistance in 3T3-L1 adipocytes.

Genipin increases mitochondrial membrane potential, ATP levels and reactive oxygen species in 3T3-L1 adipocytes

To determine whether the inhibition of UCP2 with genipin was associated with mitochondrial respiratory function in 3T3-L1 adipocytes, we measured the effect of genipin on mitochondrial membrane potential, intracellular ATP level and ROS production. As shown in Fig. 3a, addition of genipin to 3T3-L1 adipocytes apparently increased the membrane potential. An increase in mitochondrial membrane potential is predicted to stimulate ATP production by ATP synthase and increase levels of ATP. As expected, 40 μM genipin increased up to 20% ATP levels in 3T3-L1 adipocytes (Fig. 3b). Mitochondrial ROS level detected by DHR123 dye was also significantly increased in the presence of genipin (Fig. 3c). The results suggested the inhibition of UCP2 with genipin changed mitochondrial function in adipocytes. Moreover, intracellular ROS level was also significantly increased (Fig. 3d), and intracellular ROS was mainly generated from mitochondria, contributes to insulin resistance [26,27].

Inhibition of UCP2 by genipin impairs insulin signal transduction in 3T3-L1 adipocytes

To understand the mechanism by which inhibition of UCP2 induced insulin resistance in 3T3-L1 adipocytes, we examined the effect of genipin on various parameters of insulin signal transduction. Results showed a significant decrease in insulin-induced Akt phosphorylation, an important event in the insulin receptor signaling pathway (Fig. 4a). Moreover, addition of genipin to 3T3-L1 adipocytes produced a significant increase in Ser307 phosphorylation of insulin receptor substrate-1 (IRS-1) (Fig. 4b), which could lead to reduced insulin signaling [28]. Thus, inhibition of UCP2 impaired insulin signal transduction in 3T3-L1 adipocyte.

We have demonstrated that genipin increased ROS level in 3T3-L1 adipocytes. Increased ROS level are known to stimulate phosphorylation of JNK, a kinase previously linked to serine phosphorylation of IRS-1 and insulin resistance [29,30]. Our results clearly show that phosphorylation of JNK was increased in the presence of genipin (Fig. 4c).

We also use SP600125, a synthetic JNK inhibitor [31], to pretreat adipocytes with genipin. The results show inhibition of JNK activity with SP600125 could reverse the genipin-induced Ser307 phosphorylation of IRS-1 in 3T3-L1 adipocytes (Fig. 5a), and SP600125 could also largely restore the reduction of insulin-stimulated glucose uptake (Fig. 5b). These results indicate that inhibition of UCP2 by genipin in 3T3-L1 adipocytes promotes a

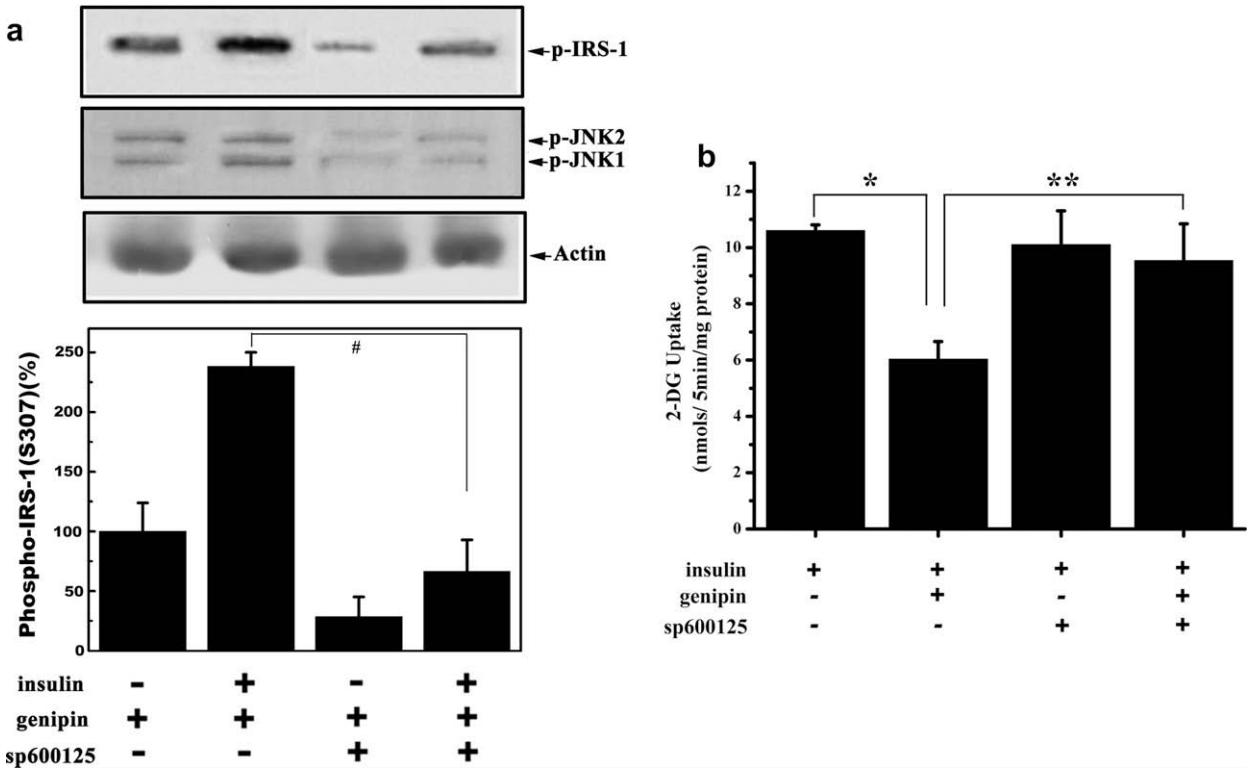

Fig. 5. JNK inhibitor could restore insulin-stimulated glucose uptake. Serum- and glucose-starved 3T3-L1 adipocytes were pretreated with 50 μM genipin for 1 h and then stimulated with 100 nM insulin as indicated. (a) Increase of Ser307 phosphorylation of IRS-1 induced by genipin was greatly reduced when cells were pretreated with genipin and additional 10 μM SP600125, a synthetic JNK inhibitor, which could largely decreased genipin-induced phosphorylation of JNK1/2. Data are shown as percentage over genipin-only condition ± SD and are representatives of three independent experiments, $^{\#}P < 0.01$. (b) As above, insulin-stimulated 2-DG uptake in adipocytes was impaired after cells were pretreated with 50 μM genipin. SP600125 could also largely restore the uptake level when cells were pretreated with additional 10 μM SP600125. 2-DG uptake was expressed as uptake amount per mg protein in 5 min. Data are the means ± SD of three independent experiments with three replicates per experiment. $^{*}P < 0.01$, $^{**}P < 0.05$.

JNK-dependent serine phosphorylation of IRS-1, which in turn inhibits insulin signal transduction and sequent glucose uptake.

Discussion

In this study, we demonstrated that inhibition of UCP2 increased mitochondrial membrane potential, intracellular ATP level and ROS production in 3T3-L1 adipocytes. Importantly, this inhibition reduced insulin-stimulated glucose uptake, indicating the involvement of UCP2 in insulin resistance in 3T3-L1 adipocytes. Inhibition of UCP2 leaded to suppression of insulin signal transduction via serine phosphorylation of IRS-1, mediated by JNK pathway.

It has been demonstrated that UCP2 is a negative regulator of insulin secretion in pancreatic β-cells [14,20]. However, it is difficult to explain the mild reduction in glycemia despite hyperinsulinemia in UCP2-null mice [20]. Recently, it was reported that increasing UCP2 levels in 3T3-L1 adipocytes are positive inducers of adiponectin (an insulin-sensitizing molecule released by adipose tissue), and therefore may favor insulin sensitivity [15]. Consistent with this finding, our results indicate that inhibition of UCP2 in 3T3-L1 adipocytes reduces glucose uptake and contributes to insulin resistance. Our results are also consistent with the findings of UCP3 occurring in skeletal muscle, i.e. overexpression of UCP3, a homolog of UCP2 in skeletal muscle has been shown to protect against fat-induced insulin resistance [16,18].

It has been evidenced that the mild regulated uncoupling caused by UCP2 and UCP3 attenuates mitochondrial ROS production, which is positively correlated with, and very sensitive to, changes in mitochondrial membrane potential [32–34], although the physiological and pathophysiological importance of UCP2 and UCP3, as a means of limiting superoxide production, is unknown. Several studies show the protective effects of overexpression of UCP2 and UCP3 [17,35,36]. Our study supports the role of UCP2 in prevention of excess ROS production as evidence that inhibition of UCP2 by genipin in 3T3-L1 adipocytes increases ROS production.

The mechanism by which inhibition of UCP2 by genipin reduces glucose uptake is undertaken. Serine phosphorylation may lead to the inhibition of IRS-1 function by promoting protein degradation of IRS-1 [37]. Our results demonstrated that inhibition of UCP2 by genipin induced the serine phosphorylation of IRS-1, which was mediated by JNK pathway, and JNK inhibitor could largely reverse the effect of genipin on serine phosphorylation of IRS-1 and insulin-stimulated glucose uptake. The activation of JNK was not clear so far. However, it has been demonstrated that increased ROS level is known to stimulate phosphorylation of JNK, which in turn induces serine phosphorylation of IRS-1 [27]. It is likely that increase of ROS resulted by inhibition of UCP2 activates the JNK signaling pathway, and contributes to the reduced glucose uptake (Fig. 6).

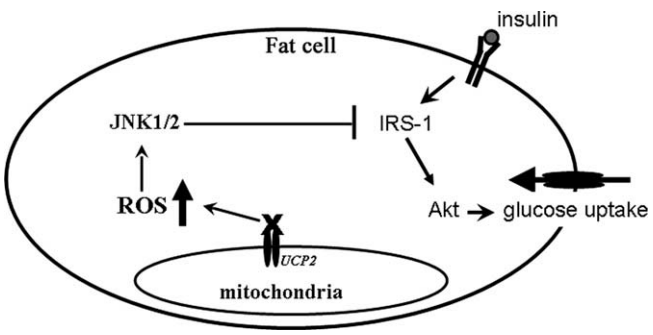

Fig. 6. Inhibition of UCP2 reduced insulin-stimulated glucose uptake in fat cell. Inhibition of UCP2 elevated intracellular ROS production, which could activate JNK1/2 pathway. JNK1/2 could increase serine phosphorylation of IRS-1, which caused impaired downstream of insulin signaling. Thus, reduced response to insulin in fat cells caused decreased glucose uptake.

In summary, these data demonstrate that inhibition of UCP2 reduces insulin-stimulated glucose uptake in 3T3-L1 adipocytes. This finding suggests that UCP2 in pancreatic β-cells and adipocytes plays different roles in the involvement of insulin resistance and systemic metabolism.

Acknowledgment

This work was supported by National Basic Research Program of China (2004CB720000 and 2006CB911001).

References

[1] A.R. Saltiel, C.R. Kahn, Nature 414 (2001) 799–806.
[2] D.B. Savage, K.F. Petersen, G.I. Shulman, Physiol. Rev. 87 (2007) 507–520.
[3] B.B. Lowell, G.I. Shulman, Science 307 (2005) 384–387.
[4] S. Krauss, C.Y. Zhang, B.B. Lowell, Nat. Rev. Mol. Cell Biol. 6 (2005) 248–261.
[5] M.D. Brand, T.C. Esteves, Cell Metab. 2 (2005) 85–93.
[6] T.C. Esteves, M.D. Brand, Biochim. Biophys. Acta 1709 (2005) 35–44.
[7] M.E. Harper, J. Himms-Hagen, Biochim. Biophys. Acta 1504 (2001) 159–172.
[8] L.P. Kozak, M.E. Harper, Annu. Rev. Nutr. 20 (2000) 339–363.
[9] C. Pecqueur, M.C. Alves-Guerra, C. Gelly, C. Levi-Meyrueis, E. Couplan, S. Collins, D. Ricquier, F. Bouillaud, B. Miroux, J. Biol. Chem. 276 (2001) 8705–8712.
[10] M. Klingenberg, K.S. Echtay, Biochim. Biophys. Acta 1504 (2001) 128–143.
[11] J. Nedergaard, V. Golozoubova, A. Matthias, A. Asadi, A. Jacobsson, B. Cannon, Biochim. Biophys. Acta 1504 (2001) 82–106.
[12] D. Arsenijevic, H. Onuma, C. Pecqueur, S. Raimbault, B.S. Manning, B. Miroux, E. Couplan, M.C. Alves-Guerra, M. Goubern, R. Surwit, F. Bouillaud, D. Richard, S. Collins, D. Ricquier, Nat. Genet. 26 (2000) 435–439.
[13] M.E. Harper, A. Antoniou, E. Villalobos-Menuey, A. Russo, R. Trauger, M. Vendemelio, A. George, R. Bartholomew, D. Carlo, A. Shaikh, J. Kupperman, E.W. Newell, I.A. Bespalov, S.S. Wallace, Y. Liu, J.R. Rogers, G.L. Gibbs, J.L. Leahy, R.E. Camley, R. Melamede, M.K. Newell, FASEB J. 16 (2002) 1550–1557.
[14] C.B. Chan, D. De Leo, J.W. Joseph, T.S. McQuaid, X.F. Ha, F. Xu, R.G. Tsushima, P.S. Pennefather, A.M. Salapatek, M.B. Wheeler, Diabetes 50 (2001) 1302–1310.
[15] E. Chevillotte, M. Giralt, B. Miroux, D. Ricquier, F. Villarroya, Diabetes 56 (2007) 1042–1050.
[16] C.S. Choi, J.J. Fillmore, J.K. Kim, Z.X. Liu, S. Kim, E.F. Collier, A. Kulkarni, A. Distefano, Y.J. Hwang, M. Kahn, Y. Chen, C. Yu, I.K. Moore, R.M. Reznick, T. Higashimori, G.I. Shulman, J. Clin. Invest. 117 (2007) 1995–2003.
[17] C.T. De Souza, E.P. Araujo, L.F. Stoppiglia, J.R. Pauli, E. Ropelle, S.A. Rocco, R.M. Marin, K.G. Franchini, J.B. Carvalheira, M.J. Saad, A.C. Boschero, E.M. Carneiro, L.A. Velloso, FASEB J. 21 (2007) 1153–1163.
[18] J.D. MacLellan, M.F. Gerrits, A. Gowing, P.J. Smith, M.B. Wheeler, M.E. Harper, Diabetes 54 (2005) 2343–2350.
[19] L.E. Parton, C.P. Ye, R. Coppari, P.J. Enriori, B. Choi, C.Y. Zhang, C. Xu, C.R. Vianna, N. Balthasar, C.E. Lee, J.K. Elmquist, M.A. Cowley, B.B. Lowell, Nature 449 (2007) 228–232.
[20] C.Y. Zhang, G. Baffy, P. Perret, S. Krauss, O. Peroni, D. Grujic, T. Hagen, A.J. Vidal-Puig, O. Boss, Y.B. Kim, X.X. Zheng, M.B. Wheeler, G.I. Shulman, C.B. Chan, B.B. Lowell, Cell 105 (2001) 745–755.
[21] C.Y. Zhang, L.E. Parton, C.P. Ye, S. Krauss, R. Shen, C.T. Lin, C.T. Lin, J.A. Porco Jr., B.B. Lowell, Cell Metab. 3 (2006) 417–427.
[22] L. Bai, Y. Wang, J. Fan, Y. Chen, W. Ji, A. Qu, P. Xu, D.E. James, T. Xu, Cell Metab. 5 (2007) 47–57.
[23] A.J. Woollacott, P.B. Simpson, J. Biomol. Screen. 6 (2001) 413–420.
[24] Y.S. Yoon, J.H. Lee, S.C. Hwang, K.S. Choi, G. Yoon, Oncogene 24 (2005) 1895–1903.
[25] A. Negre-Salvayre, N. Auge, C. Duval, F. Robbesyn, J.C. Thiers, D. Nazzal, H. Benoist, R. Salvayre, Methods Enzymol. 352 (2002) 62–71.
[26] L.E. Fridlyand, L.H. Philipson, Diabetes Obes. Metab. 8 (2006) 136–145.
[27] N. Houstis, E.D. Rosen, E.S. Lander, Nature 440 (2006) 944–948.
[28] V. Aguirre, E.D. Werner, J. Giraud, Y.H. Lee, S.E. Shoelson, M.F. White, J. Biol. Chem. 277 (2002) 1531–1537.
[29] V. Aguirre, T. Uchida, L. Yenush, R. Davis, M.F. White, J. Biol. Chem. 275 (2000) 9047–9054.
[30] J. Hirosumi, G. Tuncman, L. Chang, C.Z. Gorgun, K.T. Uysal, K. Maeda, M. Karin, G.S. Hotamisligil, Nature 420 (2002) 333–336.
[31] B.L. Bennett, D.T. Sasaki, B.W. Murray, E.C. O'Leary, S.T. Sakata, W. Xu, J.C. Leisten, A. Motiwala, S. Pierce, Y. Satoh, S.S. Bhagwat, A.M. Manning, D.W. Anderson, Proc. Natl. Acad. Sci. 98 (2001) 13681–13686.
[32] M.D. Brand, C. Affourtit, T.C. Esteves, K. Green, A.J. Lambert, S. Miwa, J.L. Pakay, N. Parker, Free Radic. Biol. Med. 37 (2004) 755–767.
[33] S.S. Korshunov, V.P. Skulachev, A.A. Starkov, FEBS Lett. 416 (1997) 15–18.
[34] A. Negre-Salvayre, C. Hirtz, G. Carrera, R. Cazenave, M. Troly, R. Salvayre, L. Penicaud, L. Casteilla, FASEB J. 11 (1997) 809–815.
[35] Z.B. Andrews, S. Diano, T.L. Horvath, Nat. Rev. Neurosci. 6 (2005) 829–840.
[36] K.U. Lee, I.K. Lee, J. Han, D.K. Song, Y.M. Kim, H.S. Song, H.S. Kim, W.J. Lee, E.H. Koh, K.H. Song, S.M. Han, M.S. Kim, I.S. Park, J.Y. Park, Circ. Res. 96 (2005) 1200–1207.
[37] M.W. Greene, H. Sakaue, L. Wang, D.R. Alessi, R.A. Roth, J. Biol. Chem. 278 (2003) 8199–8211.